Seizure 30 (2015) 124–131

Contents lists available at ScienceDirect

Seizure

journal homepage: www.elsevier.com/locate/yseiz

Extrafrontal structural changes in juvenile myoclonic epilepsy: A topographic analysis of combined structural and microstructural brain imaging

Seong Hoon Kim [a,1], Sung-Chul Lim [a,b,1], Woojun Kim [a,b], Oh-hun Kwon [c], Seun Jeon [c], Jong-Min Lee [c], Young-Min Shon [a,b,*]

[a] Department of Neurology, Seoul St. Mary's Hospital, College of Medicine, The Catholic University of Korea, 222 Banpo-daero, Seocho-gu, Seoul 137-701, Republic of Korea
[b] Catholic Neuroscience Institute, College of Medicine, The Catholic University of Korea, 222 Banpo-daero, Seocho-gu, Seoul 137-701, Republic of Korea
[c] Department of Biomedical Engineering, Hanyang University, Seoul, Republic of Korea

ARTICLE INFO

Article history:
Received 6 April 2015
Received in revised form 3 June 2015
Accepted 23 June 2015

Keywords:
Juvenile myoclonic epilepsy
Diffusion tensor imagine
Cortical thickness
Hippocampal atrophy
Water diffusivity

ABSTRACT

Purpose: An increasing amount of evidence has demonstrated that juvenile myoclonic epilepsy (JME) is associated with structural abnormalities in not only the thalamofrontal system but its adjacent regions such as temporal or parieto-occipital areas. The goal of this study was to systematically characterize morphological changes and the subsequent pathophysiological implications in JME patients using the combined structural and diffusion tensor MRI analysis.
Methods: Comparisons of white matter (WM) water diffusivity and gray matter (GM) cortical thickness were analyzed with tract-based spatial statistics (TBSS) and a Constrained Laplacian-based Anatomic Segmentation with Proximity (CLASP) algorithm, respectively. Additionally, volumes of the bilateral thalami and hippocampi were obtained using manual volumetry (MV).
Results: Compared with 22 normal controls, 18 patients with JME exhibited WM alterations in the antero-superior corona radiata, corpus callosum, both centro-parietal regions, and the left temporal lobe. JME patients also had reduced GM thickness (right paracentral lobule, precuneus, dorsolateral parietal and inferior temporal cortex; left dorsolateral frontal and anterior temporal areas). Furthermore, MV analyses revealed a significant volume reduction in the bilateral thalami and hippocampi.
Conclusions: In addition to structural changes in the thalamofrontal system, there was a conspicuous alteration of WM diffusivity in widespread extra-frontal areas and an associated decreased GM thickness in temporoparietal regions, including a significant reduction of hippocampal volume. These findings suggest that the pathophysiology of JME may be not confined to the thalamofrontal circuit but may also involve extensive areas of the extra-frontal network which encompasses temporo-parietal regions.

1. Introduction

Juvenile myoclonic epilepsy (JME) is a common type of idiopathic generalized epilepsy (IGE) that comprises approximately 8–10% of all epilepsies and is characterized by an age-specific onset of myoclonic jerks, generalized tonic–clonic seizures (GTCs), and absence seizures [1]. Seizures generally occur in the early morning or after awakening, and typical electroencephalography (EEG) findings show a 4–6 Hz rapid generalized spike-wave discharge (GSWD) pattern or a polyspike-wave discharge (SWD) pattern [2].

In general, JME patients do not appear to have structural abnormalities following conventional neuroimaging. Recently, however, several studies investigating JME patients have revealed microstructural and functional changes when using state-of-the-art imaging techniques. For example, studies using voxel-based analyses found topographical abnormalities in frontal cortical gray matter (GM) concentration and volume [3–5]. Moreover, studies using diffusion tensor imaging (DTI) or magnetic resonance spectroscopy (MRS) analyses observed changes in white matter (WM) and GM connectivity that indicated abnormal function within the thalamofrontal network in JME patients [6,7]. An emphasis on abnormal function in the frontal lobe of JME patients

* Corresponding author at: Department of Neurology, Catholic Neuroscience Institute, College of Medicine, The Catholic University of Korea, 222 Banpo-daero, Seocho-gu, Seoul 137-701, Republic of Korea. Tel.: +82 2 2258 6079; fax: +82 2 533 6079.
E-mail address: sonogung@catholic.ac.kr (Y.-M. Shon).
[1] The first two authors contribute equally to the present work.

http://dx.doi.org/10.1016/j.seizure.2015.06.009
1059-1311/

was reinforced by findings from neuropsychological testing [8] and EEG analyses [9], but several recent studies have also identified extra-frontal, focal cortical, and regional abnormalities [4,10]. Several volumetry and MRS studies revealed the hippocampal structural changes in JME, that suggest the hippocampus has important role in JME patient [11,12].

Therefore, the purpose of this study is to investigate the structural changes beyond the thalamofrontal network in JME patients. We use combined structural and microstructural neuroimaging analysis techniques to clarify the microstructural characteristics of cortical GM (surface analysis) and WM (DTI analysis) and their related subcortical structures (thalamus and hippocampus manual volumetry).

2. Methods

2.1. Subjects

This study included 18 right-handed JME patients who were followed for at least 1 year in the outpatient epilepsy clinic at Yeouido St. Mary's Hospital. All JME patients were diagnosed using the International League Against Epilepsy (ILAE) criteria for epilepsy and epileptic syndromes. The neurological exams of all patients were normal, and none of them demonstrated evidence of developmental delays or cognitive impairments on the mini-mental state examination (MMSE; score $\geq$ 28/30).

Additionally, 20 right-handed subjects with no familial or personal history of neurological, medical, or psychiatric disorders were recruited as normal controls. Control subjects were selected to exclude those without a history of seizure-like episode, syncope, head trauma or family history of epilepsy. All control subjects underwent conventional magnetic resonance imaging (MRI) and neurological examinations and did not show neurological abnormalities or have a history of drug or alcohol abuse. A board certificated radiologist and neurologist reviewed all control's brain MRI and data of neurological examination. If abnormal or unusual findings were seen on the conventional MRI or neurological exam, they were excluded. This study was approved by the local ethics committee, and all subjects provided informed consent.

2.2. MRI acquisition

Conventional MRI, DTI, and high resolution T1-weighted spoiled gradient echo (SPGR) MRI scans were obtained using a 1.5-Tesla MRI scanner (Signa Excite 11.0; GE Medical Systems; Milwaukee, WI, USA). DTI scans were acquired using a diffusion sensitizing gradient (b value = 1000 s/mm^2) along 25 directions in conjunction with axial images without diffusion weighting (b value = 0). All scans had the following characteristics: repetition time (TR) = 10,000 ms, echo time (TE) = 83.3 ms, matrix size = 128 mm $\times$ 128 mm, field of view (FOV) = 260 mm $\times$ 260 mm, number of excitations (NEX) = 1, 33 axial slices, and slice thickness = 4 mm with no inter-slice gap. For the SPGR analyses, approximately 128 adjacent axial slices parallel to the anterior–posterior commissure (AC-PC) line were obtained. All scans had the following characteristics: TR = 22 ms, TE = 6.0 ms, flip angle = 10, FOV = 256 mm $\times$ 256 mm, matrix size = 256 $\times$ 256, NEX = 1, voxel size = 0.94 mm $\times$ 0.94 mm, and slice thickness = 1.4 mm. A standard correction for field inhomogeneities was applied.

2.3. DTI processing and analysis

The raw DTI data (DICOM files) were converted to a single multivolume NIfTi file using dcm2nii software (http://www.cabiatl.com/mricro/mricron/dcm2nii.html). These DTI files were preprocessed using FMRIB's Diffusion Toolbox (FDT), a part of FSL 4.1 (http://www.fmrib.ox.ac.uk/fsl). All DTI files underwent eddy current correction for head motion correction, and the brain extraction tool (BET), a part of the FSL program, was utilized to remove non-brain structures by applying a threshold of 0.3. Subsequently, fractional anisotropy (FA) and mean diffusivity (MD) maps were generated using DTI-FIT.

A tract-based spatial statics (TBSS) algorithm, which contains the image registration and a creation of the skeleton image, was applied to analyze the data. Each skeletonized FA and MD image was then used for the voxel-wise analyses using a nonparametric test with 5000 random permutations in the "Randomise" program (http://www.fmrib.ox.ac.uk/fsl/randomise/index.html). A two sample t-test was employed for between-group comparisons with intracranial volume (ICV), age and sex treated as covariates of no interest. Statistical significance was thresholded at $p < 0.05$ and was corrected for multiple comparisons with a threshold-free cluster enhancement (TFCE).

2.4. Cortical thickness analysis

Data from one JME patient and two control subjects were excluded due to the poor quality of the SPGR images. Thus, the final sample utilized for this study was comprised of 17 JME patients and 18 normal control subjects. The MR images were first processed using the CIVET MRI analysis pipeline (version 1.1.9) that was developed at the Montreal Neurological Institute (MNI) to automatically extract and co-register the cortical surfaces for each subject. The main pipeline processing steps included the following: (1) the native three-dimensional structural MRI scan of each subject corrected for non-uniformity using the N3 algorithm, (2) brain volume classified into GM, WM, cerebrospinal fluid, and background using the INSECT algorithm, (3) the Constrained Laplacian-based Anatomic Segmentation with Proximity (CLASP) algorithm applied to generate a model of the cortical surface, which was composed of 40,962 vertices and 81,920 triangular meshes for each hemisphere, and (4) cortical thickness measured using the t-link metric, which computes the Euclidean distance between the linked vertices, respectively, of the inner and outer cortical surfaces [13]. To compare the thickness of corresponding regions between subjects, thickness values were spatially normalized using a surface-based two-dimensional registration with a sphere-to-sphere warping algorithm in which the vertices of each subject were nonlinearly registered to an average template on the sphere by matching the crowns of gyri between subjects with a crown-distance transformation. Diffusion smoothing with a full-width half-maximum (FWHM) of 20 mm was used to blur each map of cortical thickness, which increased the signal-to-noise ratio as well as the statistical power [14]. In order to analyze localized differences and the statistical map of cortical thickness on the surface model, an analysis of covariance (ANCOVA) was performed on a vertex-by-vertex basis and was corrected for multiple comparisons. Additionally, a statistical map of differences in cortical thickness between the groups was constructed using a surface model with ICV, age and gender as a covariate.

2.5. Volume measurements of the hippocampus and thalamus

The regions of interest (ROIs), which encompassed the hippocampus and thalamus, were manually outlined for segmentation using sequential oblique coronal T1-weighted MRI. The SPGR T1 sequence images were converted into cubic voxel dimensions of 0.89 mm^3 and reoriented to the hippocampal axis. The horizontal axis was parallel to a line extending from the rostral pole to the caudal pole of the hippocampus. A single expert (JH Cho) blinded to all identities and characteristics of the subjects

manually outlined the coronal hippocampus, thalamus, and the intracranial cavity (to account for inter-individual differences in brain size) contour using Analyze 10.0 (http://www.analyzedirect.com/Analyze). The margins of the hippocampus and the thalamus were defined by a persistent well-adapted protocol used in previous studies [15,16]. Repeated pilot measurements were performed in a random order on six subjects, and the intra-rater reliability was >0.974 for the right/left hippocampus and >0.963 for the right/left thalamus.

2.6. Statistical analysis

All statistical analyses comparing the two groups were performed using SPSS software (version 12.0 for windows; SPSS; Chicago, IL, USA), and all sociodemographic variables were analyzed using either a Chi-square test, Fisher's exact test, Student's *t*-test, or univariate analysis of variance (ANOVA), as appropriate. In order to account for inter-individual differences in head size, the thalamic and hippocampal volumes were corrected by dividing the intracranial volume (ICV) of each subject and then multiplying this ratio by 1,598,400 mm^3 (the average ICV of the control group). We used intracranial volume (ICV), age and sex treated as covariates of no interest. Then, a multivariate analysis of variance (MANOVA) with normalized right and left thalamic and hippocampal volumes as dependent variables and group and gender as independent variables was performed. Because the MANOVA was significant, follow-up univariate analyses were conducted. The association between the thalamic and hippocampal measurements and the sociodemographic variables were evaluated using Pearson's correlation coefficient or Spearman's rho, as appropriate. The level of statistical significance was set at $p < 0.05$ with a Bonferroni correction to allow for multiple testing. Additionally, to determine if the structural changes were related to the clinical variables, simple regression analyses were performed to establish relationships among cortical thickness, FA and MD values, hippocampal and thalamic volumes, and clinical variables (duration of epilepsy, age of onset, and frequency of seizure) in the subjects.

3. Results

3.1. Clinical characteristics

Clinical and demographic information was obtained from 18 JME patients (nine females; mean age: 23.06 ± 6.31 yrs; range: 13–38 yrs) and 20 control subjects (nine females, mean age: 25.55 ± 8.83 yrs; range: 14–40 yrs). The two groups did not differ in age or gender ($p > 0.05$; Table 1), and all patients exhibited typical EEG findings and normal conventional MRI scans. The mean age of seizure onset in the JME group was 14.6 ± 3.9 yrs (range: 7–21 yrs), and the mean duration of seizure activity was 8.3 ± 8.0 yrs (range: 1–25 yrs). All patients experienced myoclonic seizures 17 patients suffered GTC seizures (94%, frequency per year: [mean ± SD]: 3.4 ± 6.4; range: 0.1–24), and one patient experienced absence seizures (frequency per year: 52–104).

At the time of MRI acquisition, the patients were being treated with the following regimens: 11 patients were receiving only valproate, three patients were taking only levetiracetam, one patient was taking only topiramate, and three patients were taking two (two patients) or three (one patient) antiepileptic drugs (AEDs), including valproic acid (VPA).

3.2. Tract-based spatial statistics

Compared to control subjects, JME patients manifested a significant FA reduction in the deep left frontal WM and the genu, body, and isthmus of the corpus callosum (CC), both centrum semiovale, and left anterior frontal WM ($p < 0.05$, family-wise error [FWE] corrected; Fig. 1A). Additionally, widespread areas with increased MD were observed in the bilateral posterior fronto-parietal WM areas, left temporal WM and posterior part of CC ($p < 0.05$, FWE corrected; Fig. 1B). There were no areas showing increased FA or decreased MD in JME patients compared with controls.

Table 1
Clinical characteristics of JME and control subjects.

	JME patients ($n = 18$)	Control subjects ($n = 22$)	*p*-Value
Demographic and clinical data			
Age (years)	23.06 ± 6.31 (range: 13–38)	25.55 ± 8.83 (range: 14–40)	0.306
Gender (F:M)	9:9	9:13	0.577
Seizure semiology	MS (100%) GTC (94%) AS (6%)		
Age at seizure onset (years)	14.56 ± 3.93 (range: 7–21)		
Duration of epilepsy (years)	8.28 ± 8.04 (range: 1–25)		

MS, myoclonic seizure; GTC, generalized tonic clonic seizure; AS, absence seizure.

3.3. Surface based analysis of cortical thickness

JME patients exhibited a significant reduction in cortical thickness in the dorsolateral frontal cortex, anterolateral temporal cortex, and medial occipital cortices of the left hemisphere and in the paracentral lobule, precuneus, dorsolateral parietal cortex, and medial and inferior temporal cortices of the right hemisphere ($p < 0.001$, uncorrected; Fig. 2), but the clusters did not survive FWE correction. There were no regions showing increased cortical thickness.

3.4. Volume measurements of the hippocampus and thalamus

Compared with control subjects, JME patients exhibited an unwavering and significant reduction in volume in the bilateral thalami and hippocampi ($p < 0.0001$; Table 2). There was no correlation between volume loss in the thalami and hippocampi of each patient.

3.5. Correlation with clinical variables

There was no evidence of any correlation between structural changes (cortical thickness in the left and right hemispheres, FA and MD values in each hemisphere, and the volume of each side of the hippocampus and thalamus) and clinical variables (age of onset, duration of epilepsy, or frequency of myoclonic or GTC seizures; $p > 0.05$).

4. Discussion

The purpose of the present study was to investigate the structural abnormalities beyond the thalamofrontal network in JME patients and to identify the integrated structural changes of GM, WM and relevant subcortical structures, such as the thalamus and hippocampus, using T1WI and DTI techniques. There were consistent alterations of fronto-temporo-parietal microstructural WM integrity as well as cortical thinning in the corresponding GM areas. Furthermore, there was a conspicuous reduction of volume in the thalamic and hippocampal regions of JME patients compared with control subjects. To our knowledge,

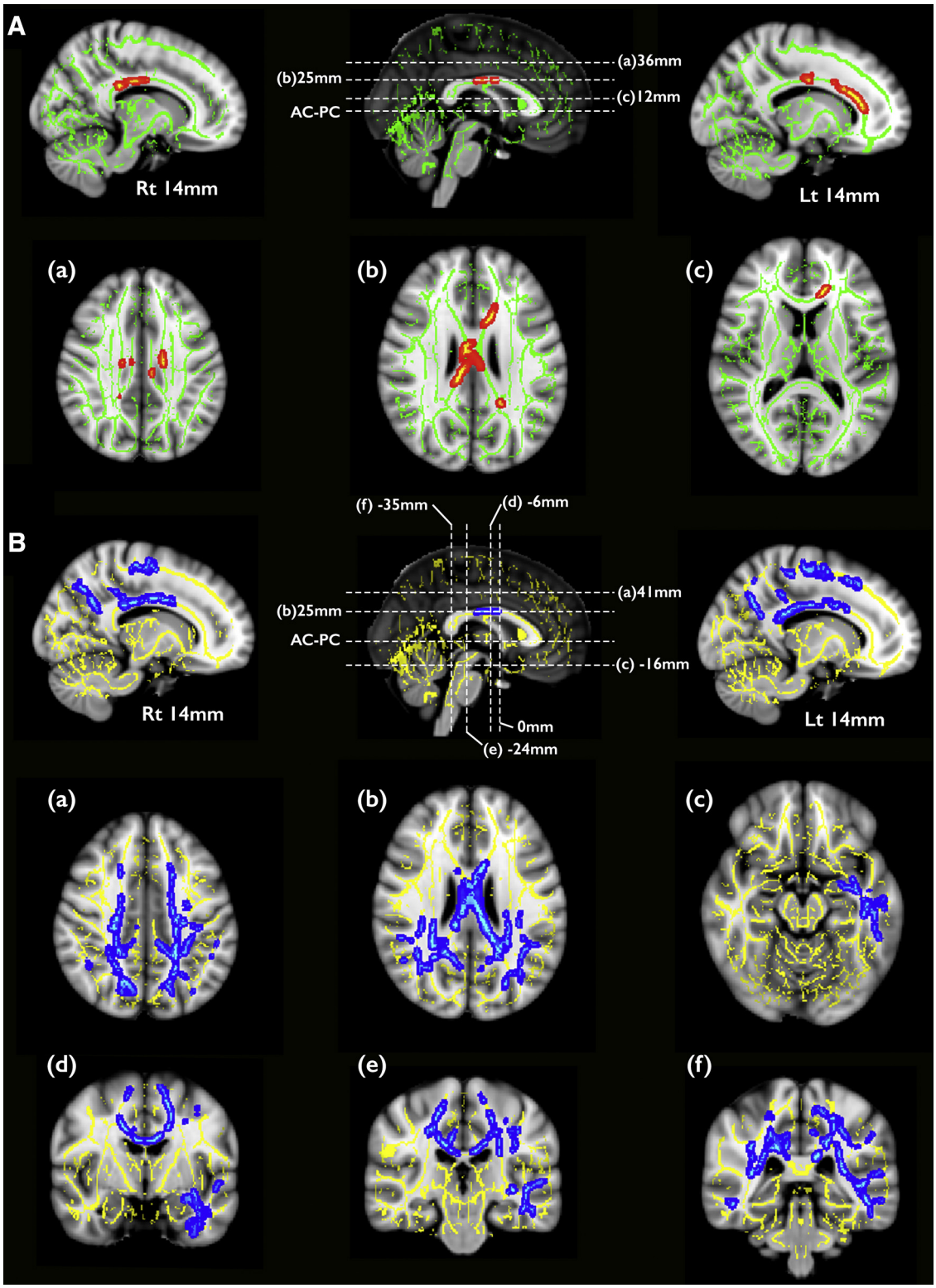

Fig. 1. Brain areas with abnormal water diffusivity analyzed by tract based spatial statics (TBSS) analysis of fraction anisotropy (FA) and mean diffusivity (MD) in JME patients. Statically significant area ($p < 0.05$, family-wise error [FWE] corrected) were seen (FA: yellow-red, MD: light blue-blue) on mean-skeletonized map (FA: green, MD: yellow). (A) The regions with reduced FA – the genu, body, and isthmus of the corpus callosum (first row), both centrum semiovale (a), and left anterior frontal WM (c). (B) Areas with increased MD – bilateral fronto-parietal WM areas (a, b and f: posteriorly predominant), left temporal WM (c, d and e), and posterior part of CC (first row).

this is the first structural imaging study demonstrating structural changes in extra-frontal WM and GM of JME patients as well as the associated subcortical core structures including the thalamus and hippocampus.

4.1. White matter abnormalities in JME patients

A number of studies have investigated changes in the water diffusivity of JME patients using whole brain voxel-wise analyses

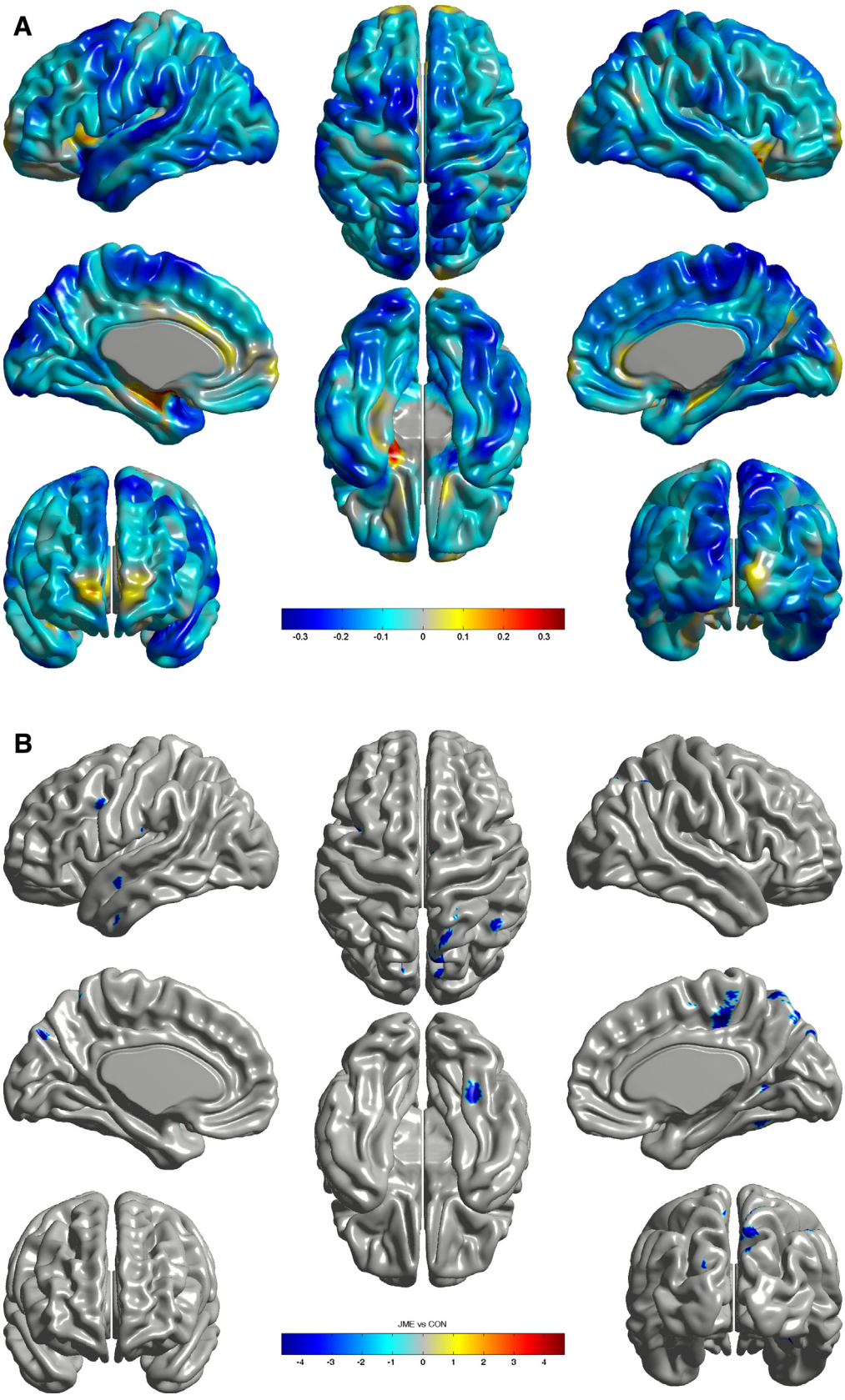

Fig. 2. Brain regions with abnormally decreased cortical thickness assessed by CLASP algorithm in JME patients. (A) Unthresholded *t*-statistics map of cortical thickness difference in JME patients relative to controls. (Blue is thinner vs. yellow to red is thicker in JME group, *t*-value indicated.) (B) Statistical threshoulded *t*-statics map ($p < 0.001$, uncorrected). In the left hemisphere, the cortical thickness was reduced in dorsolateral frontal cortex, anterolateral temporal cortex, and medial occipital cortices. In the right hemisphere, the cortical thickness was decreased in paracentral lobule, precuneus, dorsolateral parietal cortex, and medial and inferior temporal cortices.

Table 2
The normalized volume of thalamus and hippocampus in JME patients and controls measured by manual volumetry.

	JME patients ($n = 18$)	Control subjects ($n = 22$)	p-Value
Right hippocampus (mm^3)	2665.81 ± 46.37	2993.66 ± 41.89	<0.001
Left hippocampus (mm^3)	2555.56 ± 45.96	2895.68 ± 41.51	<0.001
Right thalamus (mm^3)	5912.73 ± 89.00	6539.46 ± 80.39	<0.001
Left thalamus (mm^3)	5829.92 ± 86.51	6447.02 ± 78.13	<0.001

Thalamic/hippocampal measurements was normalized to ICV and displayed in mm^3.

and found abnormal diffusivity in the anterior thalamus, prefrontal cortex, and corpus callosum [4,6]. The present findings corroborate evidence from previous studies demonstrating known pathophysiological abnormalities in the cortical networks of JME patients [10,17,18].

Interestingly, there were remarkable WM changes observed in the posterior CC (isthmus and splenium) or the posterior temporo-parietal deep WM (increased MD). However, a novel finding of this study was the identification of increased MD in temporal WM (L > R). These findings are corroborated by recent evidence of decreased FA in probabilistic temporo-parietal projections from the posterior callosal area, which indicates that there is abnormal posterior WM connectivity in JME patients [4,19]. Increased MD is known to be attributed to reduced cell number and/or volume as well as a compensatory increase in the extracellular space of WM. However, this is a non-specific measure and may be vulnerable to factors such as crossing fibers in a voxel and partial volume effects [20]. Moreover, an advanced probabilistic tracking method used in conjunction with functional MRI (fMRI) enabled the observation of increased connectivity between the medial frontal area or thalamus and the temporal neocortex, bilateral hippocampus, or amygdale [18]. This is in contrast to the decreased structural connectivity of the thalamofrontal system observed in the other studies [4,6,19]. These discrepancies may provide an explanation for increases in MD even if all fibers seem structurally or functionally intact and can prevent hasty conclusions regarding additional structural derangement in the posterior cerebral region of JME patients subsequent to sustained GSWDs. Future studies of functional connectivity using DTI tractography and fMRI analysis accompanied by corresponding neuropsychological data in JME patients may better elucidate the meaning of the present novel findings.

4.2. Cortical gray matter abnormalities in JME patients

Many studies used various methods to investigate the structural changes of cortical gray matter in JME patients. The manual volumetry is gold standard method that measures the interested structural volume by manual tracing [21]. But manual volumetry has problems of reliability and difficult to define small structure and distribution of structural changes [12,13]. MRI voxel based morphometry (VBM) uses automated analysis method, which can eliminate the investigator bias and reliability problem [22]. VBM method may provide various variables that include concentration and volume of gray matter. In VBM analysis, gray matter concentration or density means amount of gray matter around voxel. Changes of these values are still poorly understood but that suggests neuronal loss (decrease value) or cortical structural change (increase value: ex. cortical dysplasia) [3,22,23]. Previous studies of cortical GM using manual volumetry and VBM have identified subtle increases in the volume of the medial frontal cortex [5,12]. Conversely, a recent study found a reduction in GM volume in the supplementary motor area and the posterior cingulate cortex [4]. These discrepant results may be attributed to a small sample size, phenotypic heterogeneity within the sample, or the trait of inhomogeneous cortical folding, or opposing gyri in JME patients [24]. Therefore, in this study, an advanced method was used to measure the thickness of the cortical surfaces in order to differentiate between the cortices of opposing sulcal walls within the same sulcal bed, and this enabled a more precise measurement of deep sulci as well as a better analysis of the morphology of the cortical sheet [14].

The present findings not only illustrate cortical thinning in the temporal areas of JME patients but also a topographic gradient extending toward the posterior extra-frontal regions (paracentral lobule, precuneus, and parieto-occipital areas). Similar to the findings of the present study, a recent investigation using FreeSurfer, another popular imaging analysis tool, found widespread changes in cortical morphology that were related to abnormal cortical folding which encompassed the insular cortex, cingulate cortex, occipital pole, middle temporal cortex, and precuneus [10]. The same research group subsequently presented evidence of regional increases in thickness in the ventromedial frontal area as well as a number of areas within the temporal and parietal regions [17]. However, these areas did not overlap with regions showing abnormal cortical shape in their previous study [10]. This discrepancy may reflect differences in analytic methodology, but the results still support the presence of underlying microstructural changes that extend beyond the thalamofrontal regions from disease chronicity [5,25] or brain maturational alterations [26].

It is still unclear that mechanism or cause of structural change in JME. JME is common type of IGE. Some previous studies that investigated functional–structural changes of IGE provide clues to pathophysiological mechanism. Time-course analyses of the blood oxygen level dependent (BOLD) signal during GSWD have shown BOLD increments starting approximately 5–10 s prior to the onset of GSWD in the precuneus, posterior cingulate cortex, and medial/lateral parietal cortex [27]. These areas are known to play a pivotal role in generating SWDs in the thalamocortical network of patients with IGE [28]. In a recent study assessing scalp EEG sources and their causal relationships with cortical regions during SWD, the precuneus was found to play a crucial role in the onset of SWDs in the thalamofrontal cortical network as well as sustainment of the epileptic network in JME patients [29]. Another plausible explanation for the cortical thinning in these areas is associated with cortical hypoactivation that results from recurrent seizure-induced injury or the deafferentation of the cortex during GSWD, which is mediated by thalamic hyperexcitability [30]. However, in the present study, the lack of a correlation between the clinical variables of the patients and their cortical morphological traits implies that these findings are independent of seizure chronicity. Likewise, localized epileptiform discharges are frequently observed to propagate through a restricted cortical network which encompasses the frontal and temporal areas [9]. This suggests that JME can be localized, may involve cortical regions outside the frontal lobe, and may not necessarily be generalized.

4.3. Volume reduction of the hippocampus and thalamus in JME patients

The thalamus is known to be an integral component of the seizure-generating network in GSWDs [31], which is characteristic of JME, and, accordingly, gross structural changes of the thalamus have been reported in these patients [3,32]. However, the topography of the atrophy found in these studies was diverse and involved the anteromedial and posterior-dorsal nuclei [33], the anterior and right inferior nuclei [34], or the medial and lateral aspects of the bilateral thalami [35]. A possible explanation for this discordance may be differences in MR scanners or VBM

methodologies, which are vulnerable to the inaccuracy of tissue-type classification and arbitrary smoothing procedures. Another hypothesis is that JME is a genetically heterogeneous disease that has been associated with multiple gene mutations that are not universally present across diverse ethnic populations [36]. Furthermore, previous studies have been conducted using disparate groups of patients, such as those manifesting GTC seizures, myoclonic or absence seizures as the predominant seizure type of JME patients.

Importantly, the observation of overt thalamic atrophy following manual volumetry (MV) analysis added a great deal of specificity and validity relative to automated methods of measurements [16,37]. Apart from thalamic atrophy, the reduction in hippocampal volume found in the current study may support the involvement of temporal structures in JME pathophysiology. There are reciprocal anatomical connections between medial thalamic nuclei and the limbic regions [38], and experimental studies in rats with genetic absence epilepsy demonstrated limbic involvement during prevention of the full development of kindling, which demonstrates an interdependence of the temporal lobe and thalamocortical structures [39,40]. The temporal lobes, therefore, may be involved in the regulation of absence epilepsy or the resistance to the spread of SWDs in the seizure-prone limbic circuit [41].

One study using MV identified reductions in hippocampal volume and hypothesized that this is caused by the propagation of GSWDs in JME subjects [12]. Another recent study using MV in conjunction with neuropsychological testing specifically demonstrated significant hippocampal atrophy that correlated with memory dysfunction in JME patients [42]. This indicates the existence of ictogenic frontotemporal networks and supports the concept of 'system epilepsies' [43]. However, in the current study, there was not a reciprocal association between hippocampal and thalamic volume reduction, and the lack of correlation between the volume change and clinical and demographic variables in the JME patients cannot explain the exact mechanisms underlying these changes, including the cause–effect relationship between thalamic and hippocampal atrophy.

There are some limitations to this study that must be considered. First, the study sample was relatively small, and thus the lack of a significant correlation between the clinical data and the noted structural changes may result from type II error. In the future, large-sample studies are needed to confirm these results. Second, this is a cross-sectional study and, therefore, it is unclear whether these structural abnormalities are a cause or a consequence. Several studies have suggested that these findings are a consequence of recurrent seizures [4,6,44], but the converse has also been suggested [8]. Longitudinal studies may help to provide answers regarding whether the structural changes are progressive in nature or remain unchanged. Third, most patients in this cohort appear to have quite active epilepsy with frequent GTCS/year and findings may well be partially attributed to epilepsy severity – or at least this cannot be ruled out. Lastly, the necessary neuropsychological tests to measure frontal or temporal dysfunction in JME patients were not performed in this study. Previous studies have found that patients with JME have a high frequency of frontal executive dysfunction [6,8] as well as verbal or visual memory dysfunction associated with decreased hippocampal or temporal neural activity [42,45]. Importantly, the present findings demonstrate specific novel structural abnormalities in the temporoparietal regions of JME patients. However, a reciprocal abnormal functional connectivity within the thalamocortical network that may underlie the clinical and neuropsychological alterations in JME patients cannot be demonstrated by the present findings. Therefore, further prospective studies investigating anatomical, electrophysiological, pharmacological, and neuropsychological data from de novo and existing JME patients are necessary.

In conclusion, the use of combined imaging analyses in this study demonstrated widespread structural abnormalities in JME patients, with an emphasis on the limbic and temporoparietal regions. Our results suggest that structural MRI changes of JME may be widespread, rather than confined to well-known frontothalamic circuit. The precise implication of these findings and these specific brain regions is not yet known, and further investigation, including neurocognitive evaluations, is warranted in the near future.

Conflicts of interest

The authors have no conflicts of interest to disclose.

Acknowledgments

This study was supported by a grant of the Korean Health Technology R&D Project, Ministry for Health, Welfare and Family Affairs, Republic of Korea (grant number A092125). We confirm that we have read the Journal's position on issues involved in ethical publication and affirm that this report is consistent with those guidelines.

References

[1] Janz D. Epilepsy with impulsive petit mal (juvenile myoclonic epilepsy). Acta Neurol Scand 1985;72:449–59.
[2] Pedersen SB, Petersen KA. Juvenile myoclonic epilepsy: clinical and EEG features. Acta Neurol Scand 1998;97:160–3.
[3] Betting LE, Mory SB, Li LM, Lopes-Cendes I, Guerreiro MM, Guerreiro CA, et al. Voxel-based morphometry in patients with idiopathic generalized epilepsies. Neuroimage 2006;32:498–502.
[4] O'Muircheartaigh J, Vollmar C, Barker GJ, Kumari V, Symms MR, Thompson P, et al. Focal structural changes and cognitive dysfunction in juvenile myoclonic epilepsy. Neurology 2011;76:34–40.
[5] Woermann FG, Free SL, Koepp MJ, Sisodiya SM, Duncan JS. Abnormal cerebral structure in juvenile myoclonic epilepsy demonstrated with voxel-based analysis of MRI. Brain 1999;122(Pt 11):2101–8.
[6] Kim JH, Suh SI, Park SY, Seo WK, Koh I, Koh SB, et al. Microstructural white matter abnormality and frontal cognitive dysfunctions in juvenile myoclonic epilepsy. Epilepsia 2012;53:1371–8.
[7] Lin K, Carrete Jr H, Lin J, Peruchi MM, de Araujo Filho GM, Guaranha MS, et al. Magnetic resonance spectroscopy reveals an epileptic network in juvenile myoclonic epilepsy. Epilepsia 2009;50:1191–200.
[8] Pulsipher DT, Seidenberg M, Guidotti L, Tuchscherer VN, Morton J, Sheth RD, et al. Thalamofrontal circuitry and executive dysfunction in recent-onset juvenile myoclonic epilepsy. Epilepsia 2009;50:1210–9.
[9] Holmes MD, Quiring J, Tucker DM. Evidence that juvenile myoclonic epilepsy is a disorder of frontotemporal corticothalamic networks. Neuroimage 2010;49:80–93.
[10] Ronan L, Alhusaini S, Scanlon C, Doherty CP, Delanty N, Fitzsimons M. Widespread cortical morphologic changes in juvenile myoclonic epilepsy: evidence from structural MRI. Epilepsia 2012;53:651–8.
[11] Ristic AJ, Ostojic J, Kozic D, Vojvodic NM, Popovic LM, Jankovic S, et al. Hippocampal metabolic dysfunction in juvenile myoclonic epilepsy: 3D multi-voxel spectroscopy study. J Neurol Sci 2011;305:139–42.
[12] Tae WS, Hong SB, Joo EY, Han SJ, Cho JW, Seo DW, et al. Structural brain abnormalities in juvenile myoclonic epilepsy patients: volumetry and voxel-based morphometry. Korean J Radiol 2006;7:162–72.
[13] Lerch JP, Evans AC. Cortical thickness analysis examined through power analysis and a population simulation. Neuroimage 2005;24:163–73.
[14] Im K, Lee JM, Lee J, Shin YW, Kim IY, Kwon JS, et al. Gender difference analysis of cortical thickness in healthy young adults with surface-based methods. Neuroimage 2006;31:31–8.
[15] Natsume J, Bernasconi N, Andermann F, Bernasconi A. MRI volumetry of the thalamus in temporal, extratemporal, and idiopathic generalized epilepsy. Neurology 2003;60:1296–300.
[16] Pruessner JC, Li LM, Serles W, Pruessner M, Collins DL, Kabani N, et al. Volumetry of hippocampus and amygdala with high-resolution MRI and three-dimensional analysis software: minimizing the discrepancies between laboratories. Cereb Cortex 2000;10:433–42.
[17] Alhusaini S, Ronan L, Scanlon C, Whelan CD, Doherty CP, Delanty N, et al. Regional increase of cerebral cortex thickness in juvenile myoclonic epilepsy. Epilepsia 2013;54:e138–41.
[18] O'Muircheartaigh J, Vollmar C, Barker GJ, Kumari V, Symms MR, Thompson P, et al. Abnormal thalamocortical structural and functional connectivity in juvenile myoclonic epilepsy. Brain 2012;135:3635–44.

[19] Focke NK, Diederich C, Helms G, Nitsche MA, Lerche H, Paulus W. Idiopathic-generalized epilepsy shows profound white matter diffusion-tensor imaging alterations. Hum Brain Mapp 2014;35:3332–42.
[20] Jbabdi S, Behrens TE, Smith SM. Crossing fibres in tract-based spatial statistics. Neuroimage 2010;49:249–56.
[21] Allen JS, Damasio H, Grabowski TJ. Normal neuroanatomical variation in the human brain: an MRI-volumetric study. Am J Phys Anthropol 2002;118:341–58.
[22] Whitwell JL. Voxel-based morphometry: an automated technique for assessing structural changes in the brain. J Neurosci 2009;29:9661–4.
[23] Mechelli A, Price CJ, Friston KJ, Ashburner J. Voxel-based morphometry of the human brain: methods and applications. Curr Med Imaging Rev 2005;1:105–13.
[24] Anderson J, Hamandi K. Understanding juvenile myoclonic epilepsy: contributions from neuroimaging. Epilepsy Res 2011;94:127–37.
[25] Tae WS, Kim SH, Joo EY, Han SJ, Kim IY, Kim SI, et al. Cortical thickness abnormality in juvenile myoclonic epilepsy. J Neurol 2008;255:561–6.
[26] Lin JJ, Dabbs K, Riley JD, Jones JE, Jackson DC, Hsu DA, et al. Neurodevelopment in new-onset juvenile myoclonic epilepsy over the first 2 years. Ann Neurol 2014;76:660–8.
[27] Benuzzi F, Mirandola L, Pugnaghi M, Farinelli V, Tassinari CA, Capovilla G, et al. Increased cortical BOLD signal anticipates generalized spike and wave discharges in adolescents and adults with idiopathic generalized epilepsies. Epilepsia 2012;53:622–30.
[28] Vaudano AE, Laufs H, Kiebel SJ, Carmichael DW, Hamandi K, Guye M, et al. Causal hierarchy within the thalamo-cortical network in spike and wave discharges. PLoS ONE 2009;4:e6475.
[29] Lee C, Kim S-M, Jung Y-J, Im C-H, Kim DW, Jung K-Y. Causal influence of epileptic network during spike-and-wave discharge in juvenile myoclonic epilepsy. Epilepsy Res 2014;108(February (2)):257–66.
[30] Gotman J, Grova C, Bagshaw A, Kobayashi E, Aghakhani Y, Dubeau F. Generalized epileptic discharges show thalamocortical activation and suspension of the default state of the brain. Proc Natl Acad Sci U S A 2005;102:15236–40.
[31] Blumenfeld H. Cellular and network mechanisms of spike-wave seizures. Epilepsia 2005;46(Suppl. 9):21–33.
[32] Kim JH, Lee JK, Koh SB, Lee SA, Lee JM, Kim SI, et al. Regional grey matter abnormalities in juvenile myoclonic epilepsy: a voxel-based morphometry study. Neuroimage 2007;37:1132–7.
[33] Kim JH, Kim JB, Seo WK, Suh SI, Koh SB. Volumetric and shape analysis of thalamus in idiopathic generalized epilepsy. J Neurol 2013;260:1846–54.
[34] Mory SB, Betting LE, Fernandes PT, Lopes-Cendes I, Guerreiro MM, Guerreiro CA, et al. Structural abnormalities of the thalamus in juvenile myoclonic epilepsy. Epilepsy Behav 2011;21:407–11.
[35] Saini J, Sinha S, Bagepally BS, Ramchandraiah CT, Thennarasu K, Prasad C, et al. Subcortical structural abnormalities in juvenile myoclonic epilepsy (JME): MR volumetry and vertex based analysis. Seizure 2013;22:230–5.
[36] Velisek L, Shang E, Veliskova J, Chachua T, Macchiarulo S, Maglakelidze G, et al. GABAergic neuron deficit as an idiopathic generalized epilepsy mechanism: the role of BRD2 haploinsufficiency in juvenile myoclonic epilepsy. PLoS ONE 2011;6:e23656.
[37] Cocosco CA, Zijdenbos AP, Evans AC. A fully automatic and robust brain MRI tissue classification method. Med Image Anal 2003;7:513–27.
[38] Zhang DX, Bertram EH. Midline thalamic region: widespread excitatory input to the entorhinal cortex and amygdala. J Neurosci 2002;22:3277–84.
[39] Carcak N, Ferrandon A, Koning E, Aker RG, Ozdemir O, Onat FY, et al. Effect of stage 2 kindling on local cerebral blood flow rates in rats with genetic absence epilepsy. Epilepsia 2009;50:33–43.
[40] Onat FY, Aker RG, Gurbanova AA, Ates N, van Luijtelaar G. The effect of generalized absence seizures on the progression of kindling in the rat. Epilepsia 2007;48(Suppl. 5):150–6.
[41] Nehlig A, Vergnes M, Marescaux C, Boyet S, Lannes B. Local cerebral glucose utilization in rats with petit mal-like seizures. Ann Neurol 1991;29:72–7.
[42] Lin K, de Araujo Filho GM, Pascalicchio TF, Silva I, Tudesco IS, Guaranha MS, et al. Hippocampal atrophy and memory dysfunction in patients with juvenile myoclonic epilepsy. Epilepsy Behav 2013;29:247–51.
[43] Avanzini G, Manganotti P, Meletti S, Moshe SL, Panzica F, Wolf P, et al. The system epilepsies: a pathophysiological hypothesis. Epilepsia 2012;53:771–8.
[44] Deppe M, Kellinghaus C, Duning T, Moddel G, Mohammadi S, Deppe K, et al. Nerve fiber impairment of anterior thalamocortical circuitry in juvenile myoclonic epilepsy. Neurology 2008;71:1981–5.
[45] Kim SY, Hwang YH, Lee HW, Suh CK, Kwon SH, Park SP. Cognitive impairment in juvenile myoclonic epilepsy. J Clin Neurol 2007;3:86–92.